PHYSICAL REVIEW E **91**, 021001(R) (2015)

Pair dispersion of turbulent premixed flame elements

Swetaprovo Chaudhuri*
Department of Aerospace Engineering, National Center for Combustion Research and Development, Indian Institute of Science, Bangalore 560012, India
(Received 20 November 2014; published 26 February 2015)

Flame particles are mathematical points comoving with a reacting isoscalar surface in a premixed flame. In this Rapid Communication, we investigate mean square pair separation of flame particles as a function of time from their positions tracked in two sets of direct numerical simulation solutions of H_2-air turbulent premixed flames with detailed chemistry. We find that, despite flame particles and fluid particles being very different concepts, a modified Batchelor's scaling of the form $\langle|\mathbf{\Delta}^F(t)-\mathbf{\Delta}^F(0)|^2\rangle = C_F(\langle\varepsilon\rangle_0^F\,\Delta_0^F)^{2/3}t^2$ holds for flame particle pair dispersion. The proportionality constant, however, is not universal and depends on the isosurface temperature value on which the flame particles reside. Following this, we attempt to analytically investigate the rationale behind such an observation.

DOI: 10.1103/PhysRevE.91.021001 PACS number(s): 47.70.Pq, 47.27.Gs

I. INTRODUCTION

One of the few roots of modern turbulence research could be traced back to the works of Taylor [1] and Richardson [2] who studied single particle dispersion and particle pair dispersion, respectively. Inherently, the pair dispersion problem is coupled to turbulent mixing and diffusion, thus finding wide applications in studies on spreading and mixing of chemical species in the ocean or atmosphere. Defining the pair separation distance vector $\mathbf{\Delta} = \mathbf{X}_i - \mathbf{X}_j$, where $\mathbf{X}_i, \mathbf{X}_j$ are the position vectors of the two particles, respectively, Richardson modeled $q(s,t)$: the probability density function (PDF) of $\Delta = |\mathbf{\Delta}|$, in the inertial range by the following diffusion equation:

$$\frac{\partial q(s,t)}{\partial t} = \frac{1}{s^{(d-1)}}\frac{\partial}{\partial s}\left[K(s)s^{(d-1)}\frac{\partial q(s,t)}{\partial s}\right], \tag{1}$$

where s is the sample space variable corresponding to Δ, d is the spatial dimension, and $K(s)$ is the scale dependent pair dispersion coefficient with dimension $[L^2T^{-1}]$ as reviewed in [3]. The moments of Δ are given by

$$\langle\Delta^p(t)\rangle = \int_0^\infty s^p q(s,t)4\pi s^2 ds. \tag{2}$$

The effective eddy diffusion coefficient could be defined as

$$K_{\text{eff}} = \frac{1}{2d}\frac{d\langle\Delta^2(t)\rangle}{dt}. \tag{3}$$

Richardson [2] found $K_{\text{eff}} \sim \langle\Delta^2(t)\rangle^{2/3}$, which was used to obtain what is now known as Richardson's 4/3 law: $K(s) = C_R s^{4/3}$, where C_R is a dimensional constant later obtained by Obukhov [4] as $C_R = k_0\langle\varepsilon\rangle^{1/3}$, where k_0 is a dimensionless constant and $\langle\varepsilon\rangle$ is the mean energy dissipation rate. Solving for Eq. (1), using the 4/3 law, the "superdiffusive" behavior of a particle pair in turbulence was predicted by the following equation known as the Richardson-Obukhov (R-O) law:

$$\langle\Delta^2(t)\rangle = g\,\langle\varepsilon\rangle\,t^3. \tag{4}$$

Using the K41 theory of turbulence [5], Batchelor [6] obtained two scaling laws for pair dispersion valid in the small time and large time limit, respectively, and are given by

$$\langle|\mathbf{\Delta}(t)-\mathbf{\Delta}_0|^2\rangle = \frac{11}{3}C_2(\langle\varepsilon\rangle\,\Delta_0)^{2/3}t^2 \quad \text{while} \quad t \ll t_0 = \left(\frac{\Delta_0^2}{\langle\varepsilon\rangle}\right)^{1/3} \tag{5}$$

and

$$\langle|\mathbf{\Delta}(t)-\mathbf{\Delta}_0|^2\rangle = \tfrac{1144}{81}k_0^3\,\langle\varepsilon\rangle\,t^3 \quad \text{for} \quad t_0 \ll t \ll t_L, \tag{6}$$

where $\mathbf{\Delta}_0 = \mathbf{\Delta}(t=0)$, and t_0 and t_L are the Batchelor time scale and the Lagrangian integral time scale, respectively. C_2 is the Kolmogorov constant = 2.13 [7]. The short time limit scaling of pair dispersion [Eq. (5)] has been recently verified in [8] using rigorous particle tracking experiments.

In turbulent premixed combustion, the concept of turbulent eddy diffusivity is of paramount importance and was used by Damköhler [9] for modeling turbulent flame speed; in Reynolds Averaged Navier Stokes (RANS) modeling of progress variable formulation [10] or as summarized in [11] in the context of modeling turbulent flame brush thickness. Nevertheless, in turbulent premixed combustion, Lagrangian description is rare except in the pioneering theoretical and computational studies by Pope and co-workers [12,13]. At that time detailed chemistry turbulent combustion direct numerical simulation (DNS) was impossible with state of the art computational resources, and computations on surface points were performed in nonreacting isothermal homogeneous isotropic turbulence (NRIHIT) with a constant or linear flame speed model [14].

Recently, we used the surface point concept in DNS solutions of turbulent premixed flames with detailed chemistry to obtain Lagrangian tracking of flame elements or flame particles [15]. Here, flame particles are surface points that comove with a given reacting isoscalar surface within a premixed flame. Thus flame particles follow an isosurface in a premixed flame by always residing on the isosurface and are distinctly different from fluid particles which would pass through a premixed flame. Following the notation used in [12], the flame particle's position vector at a time t is denoted by $\mathbf{X}^F(t)$ with its motion given by

$$\mathbf{V}^F(t) = \frac{d}{dt}\mathbf{X}^F(t) = \mathbf{U}(\mathbf{X}^F[t],t) + S_d(\mathbf{X}^F[t],t)\mathbf{n}^F(\mathbf{X}^F[t],t). \tag{7}$$

*schaudhuri@aero.iisc.ernet.in; swetaprovo@gmail.com

TABLE I. Simulation Parameters.

Case	$\langle U\rangle$	L_I	τ_I	η	τ_η	$u_{\rm rms}$	$S_{L,0}\,(T=310\ {\rm K})$	$S_{L,0}\,(T=500\ {\rm K})$	δ_L	Δ(grid size)	$\tau_{\rm Track}$	$\Delta\tau_{\rm Track}$
A	500 cm/s	0.109 cm	217 μs	17 μm	14 μs	503 cm/s	185 cm/s	284 cm/s	361 μm	39.0625 μm	292 μs	2.5 μs
B	700 cm/s	0. 074 cm	133 μs	15 μm	10 μs	557 cm/s	185 cm/s	284 cm/s	361 μm	31.250 μm	208 μs	2.5 μs

Here $\mathbf{U}(\mathbf{X}^F[t],t)$ is the flow velocity at $\mathbf{X}^F(t)$; $S_d(\mathbf{X}^F[t],t)$ being the local displacement flame speed and $\mathbf{n}^F(\mathbf{X}^F[t],t)$ the local surface normal at $\mathbf{X}^F(t)$. It is well known that $S_d \sim \sqrt{\alpha\dot{\omega}}$, where α and $\dot{\omega}$ are the thermal diffusivity and reaction rate with additional dependence on local strain rate and curvature [16]. Essentially, a Lagrangian technique for analyzing turbulent premixed flame motion from DNS solutions was established in [15] and could be immediately applied to the problem of flame particle pair dispersion. To delineate between fluid particle and flame particle pair dispersion we define the latter as $\mathbf{\Delta}^F = \mathbf{X}_i^F - \mathbf{X}_j^F$, where $\mathbf{X}_i^F, \mathbf{X}_j^F$ are the position vectors of the ith and jth flame particles, respectively. The presence of a premixed flame causes gas expansion and flow acceleration. Thus, local isotropy is lost within a premixed flame in an otherwise homogeneous isotropic turbulence. It is, however, crucial to investigate flame particle pair dispersion as that would elucidate how flame surface fluctuations disperse, diffuse, and propagate in a turbulent flow field: processes ubiquitous in SI engines, gas turbine engines, or supernova explosions. In this Rapid Communication, we will first attempt to demonstrate a possible scaling of flame particle pair dispersion, applying flame particle tracking (FPT) in two DNS solutions of H_2-air turbulent premixed flames. Following this, we will attempt to analytically derive the scaling for flame particle pair dispersion by an approach very similar to that by Batchelor [6] for fluid particles.

II. COMPUTATIONS

Two DNS cases (cases A and B) were performed with the PENCIL code for lean H_2-air premixed flames with detailed chemical reaction mechanism of [17]. PENCIL code is an open source code designed for compressible turbulent flows using sixth order finite difference and third order Runge-Kutta schemes for spatial and temporal discretization, respectively. Combustion chemistry was implemented in [18]. The well-known axial inlet-outlet flow configuration with periodic boundary conditions on the sides was used for simulating a near statistically stationary and planar turbulent premixed flame within a rectangular box of size 1 cm $\times$ 0.5 cm $\times$ 0.5 cm for case A, corresponding to a grid size of 256 $\times$ 128 $\times$ 128 grid points. Homogeneous isotropic turbulence solution was fed in through the inlet with a superimposed mean flow in the axial direction with upstream turbulence Reynolds number $\mathrm{Re}_T = 252$ and Damköhler number ($\mathrm{Da} = L_{I,\mathrm{inlet}} S_{L,0}/u_{\mathrm{rms,inlet}}\delta_{L,0}$) $\mathrm{Da} = 1.10$ for case A. For case B, the rectangular box size was set at 1.2 cm $\times$ 0.4 cm $\times$ 0.4 cm within a grid of 384 $\times$ 128 $\times$ 128 points with $\mathrm{Re}_T = 198$ and $\mathrm{Da} = 0.68$. Further details about cases A and B could be found in Table I. Results on evolution of strain rate and curvature from case A and further details of the computations, algorithms, and DNS results could be found in [15]. Case B DNS has been newly performed for exploring flame particle pair dispersion in the context of flames deep within the thin reaction regime. FPT was performed in the postprocessing mode using ray tracing and ray-face intersection techniques, which yields flame particle positions at sub-Kolmogorov time scale intervals over the tracking time. These positions could be used for probing flame particle pair dispersion, which has never been addressed, to our knowledge. Visualization of the motion of all the flame particles for both cases and relative dispersion for a particular pair belonging to the $T = 500$ K isosurface in case A, can be found in the Supplemental Material [19].

III. RESULT AND DISCUSSIONS

Figures 1(a)–1(d) and 2(a)–2(d) show the results of flame particle pair dispersion obtained from the DNS and FPT for cases A and B, respectively. In the FPT, flame particles were injected on $T = 500$ K and $T = 1000$ K isosurfaces, respectively, at a time instant when the flame was moderately wrinkled by oncoming turbulence. We will consider this time instant as $t = 0$. Only pair dispersions among flame particles belonging to a given isosurface are considered. In practice, this was accomplished by choosing the ith flame particle as a reference and computing the vector $\mathbf{\Delta} = \mathbf{X}_i^F - \mathbf{X}_j^F$ from the ith to all other j flame particles. Then this process was repeated for all j flame particles for $j > i$. This resulted in 125250 flame particle pairs with initial separation distance Δ_0^F ranging from nearly the Kolmogorov length scale to the domain size along the diagonal.

It was recognized in [15] that due to inherent flame surface fluctuation dissipation mechanisms such as kinematic restoration [20], Markstein diffusion [21], and island formation, a flame particle has a finite lifetime denoted by $\tau_{F,L}$ unlike a fluid particle which has an infinite lifetime. The relative dispersion tracking for a given pair was therefore performed till any member of that pair gets lost due to the annihilation of its resident surface.

Figures 1(a) and 1(b) show the scaled, mean of pair separation distance squared: $\langle|\mathbf{\Delta}^F(t) - \mathbf{\Delta}_0^F|^2\rangle_r/[\frac{11}{3}C_2(\langle\varepsilon\rangle_0^F\Delta_0^F)^{2/3}]$ versus t for flame particle pairs separated within the inertial range $50\eta \leqslant \Delta_0^F \leqslant 242\eta$ belonging to $T = 500$ K and $T = 1000$ K isosurfaces, respectively, for case A. $\langle\varepsilon\rangle_0^F$ is the energy dissipation rate averaged over the corresponding isosurface on which the flame particles were embedded, at $t = 0$ s. Such a scaling is considered to check the validity of Eq. (5) in the context of flame particles. First, flame particle pairs with $50\eta \leqslant \Delta_0^F \leqslant 242\eta$ were sorted into 100 bins based on their initial separation Δ_0^F. $|\mathbf{\Delta}^F(t) - \mathbf{\Delta}_0^F|^2$ were averaged over individual bins denoted by $\langle\rangle_r$, followed by scaling and plotting with t to produce the individual curves shown in Figs. 1(a) and 1(b). In both Figs. 1(a) and 1(b) we see that the data corresponding to different initial separations nearly collapse on a single straight line. Hence it is possible that, for flame particles $\langle|\mathbf{\Delta}^F(t) - \mathbf{\Delta}_0^F|^2\rangle_r/[\frac{11}{3}C_2(\langle\varepsilon\rangle_0^F\Delta_0^F)^{2/3}] \sim t^2$ similar to Batchelor scaling, i.e., Eq. (5) for fluid particles. These results are not intuitive as flame particles considered here

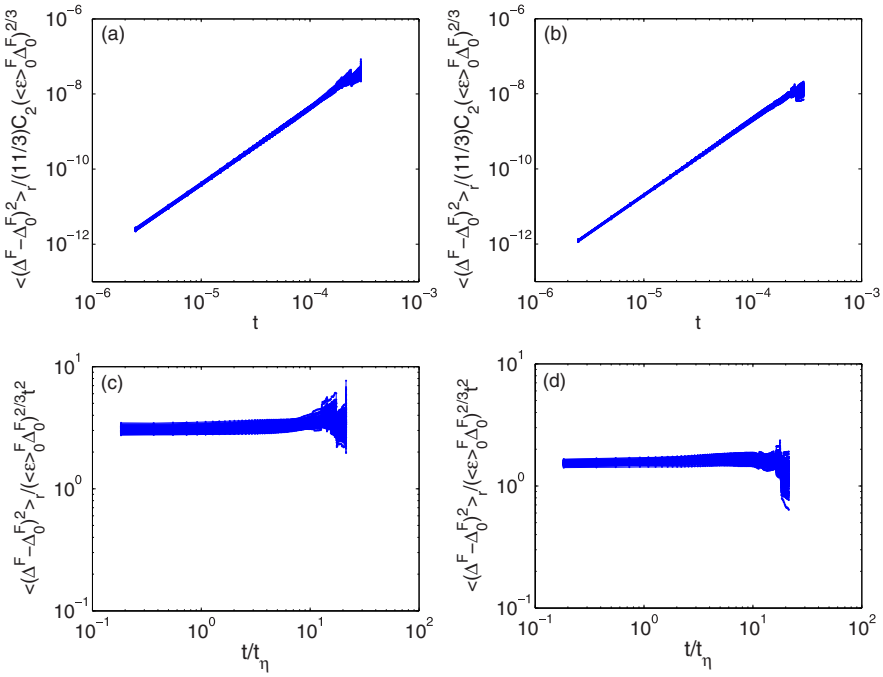

FIG. 1. (Color online) Scaled, mean squared flame particle pair separation vs time in seconds for flame particles belonging to the isosurface (a) $T = 500$ K and (b) $T = 1000$ K for case A. Compensated mean squared flame particle pair separation vs time normalized with Kolmogorov time scale for flame particles belonging to the isosurface (c) $T = 500$ K and (d) $T = 1000$ K for case A.

reside on reacting isosurfaces accompanied by heat release and dilatation which would render the flow locally anisotropic. Though $(u_{\rm rms}/S_d)_{T=T_0}$, heat release rate and dilatation are quite different at the two isosurfaces: $T = 500$ K and $T = 1000$ K, they do not greatly affect the pair dispersion scaling. The $(u_{\rm rms}/S_{d,0})_{T=T_0}$ varies within $1 \leqslant (u_{\rm rms}/S_{d,0})_{T=500\ {\rm K}} \leqslant 1.8$ and $0.5 \leqslant (u_{\rm rms}/S_{d,0})_{T=1000\ {\rm K}} \leqslant 1$ over the entire tracking time. Of course, due to density effects: $S_{d,0@T=1000\ {\rm K}} > S_{d,0@T=500\ {\rm K}}$. However, $(u_{\rm rms}/S_{d,0})_{T=T_0} \sim O(1)$ precludes the hypothesis that the current observation is an artifact of asymptotic passive scalar behavior when $u_{{\rm rms},{\rm T}_0} \gg S_{d_0,T_0}$. Clearly, the flame particle and fluid particle motions are not synonymous due to the inherent displacement flame speed, i.e., the second term of Eq. (7) arising out of diffusion and reaction in a premixed flame. S_d directed normal to the surface ($S_d\mathbf{n}$) changes both the magnitude and direction of the flame particle motion with respect to the velocity of a fluid particle sharing the same position at the same time instant. Such differences are, however, manifested in the pair dispersion scaling of Figs. 1(a) and 1(b): not in the exponent but in the proportionality constants. To explore this further, we plot the compensated scaling of $\langle|\mathbf{\Delta}^F(t) - \mathbf{\Delta}_0^F|^2\rangle_r/[(\langle\varepsilon\rangle_0^F\Delta_0^F)^{2/3}t^2]$ versus t/t_η in Figs. 1(c) and 1(d) for $T = 500$ K and $T = 1000$ K, respectively. We clearly see that the data collapse on a horizontal narrow band proving that indeed, $\langle|\mathbf{\Delta}^F(t) - \mathbf{\Delta}_0^F|^2\rangle_r \sim (\langle\varepsilon\rangle_0^F\Delta_0^F)^{2/3}t^2$. The proportionality constants are nearly 3.0 and 1.5 in Figs. 1(c) and 1(d) for $T = 500$ K and $T = 1000$ K,

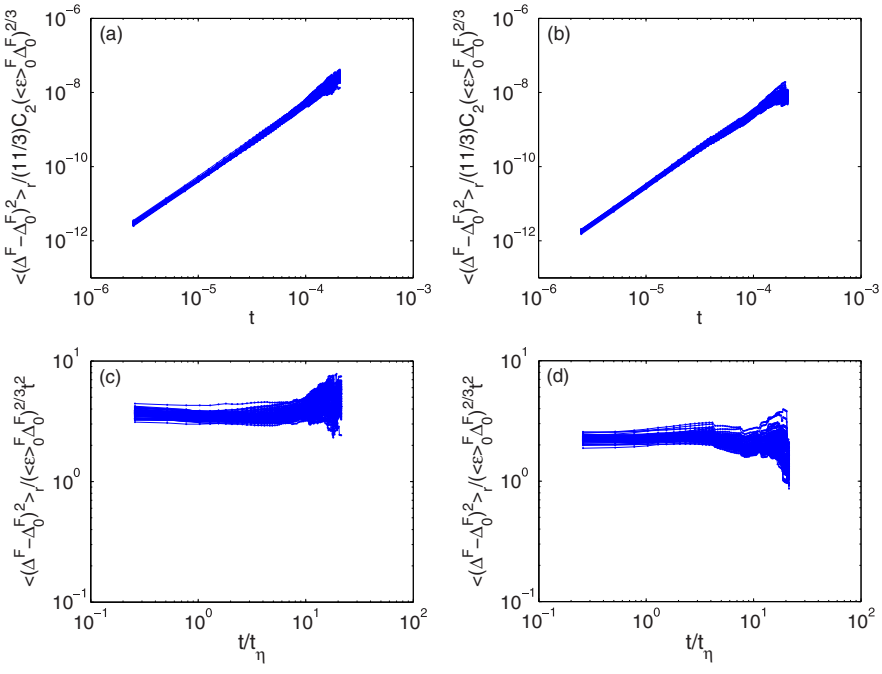

FIG. 2. (Color online) Scaled, mean squared flame particle pair separation vs time in seconds for flame particles belonging to the isosurface (a) $T = 500$ K and (b) $T = 1000$ K for case B. Compensated mean squared flame particle pair separation vs time normalized with Kolmogorov time scale for flame particles belonging to the isosurface (c) $T = 500$ K and (d) $T = 1000$ K for case B.

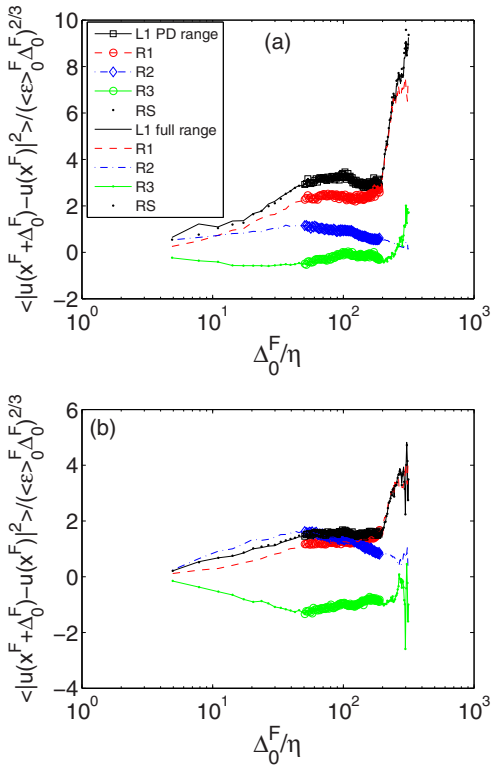

FIG. 3. (Color online) Compensated structure functions for case A corresponding to different terms of Eq. (15) at $t = 0$ for (a) $T = 500$ K and (b) $T = 1000$ K. The symbols represent the range of $50\eta \leqslant \Delta_0^F \leqslant 242\eta$ which was used for flame particle pair dispersion (PD) scaling reported in Figs. 1(a)–1(d).

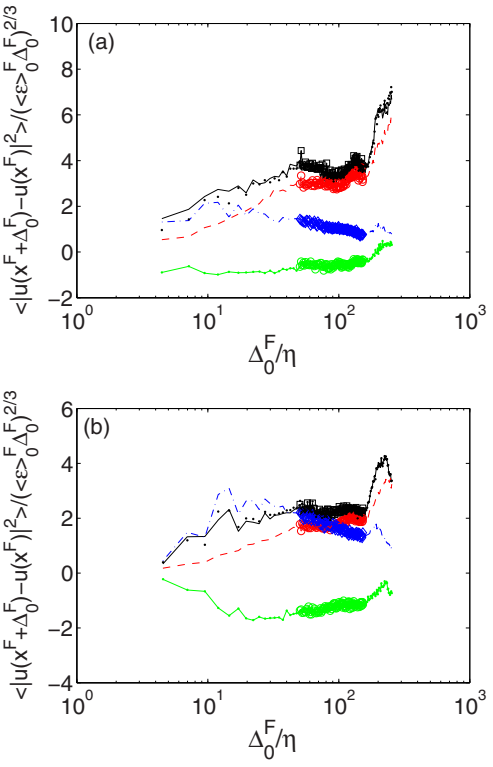

FIG. 4. (Color online) Compensated structure functions for case B corresponding to different terms of Eq. (15) at $t = 0$ for (a) $T = 500$ K and (b) $T = 1000$ K. The symbols represent the range of $50\eta \leqslant \Delta_0^F \leqslant 200\eta$ which was used for flame particle pair dispersion (PD) scaling reported in Figs. 2(a)–2(d).

respectively. In NRIHIT the corresponding proportionality constant for fluid particles is $11C_2/3 = 7.81$. Case B results are shown in Figs. 2(a) and 2(b), which show the scaled, mean of pair separation distance squared: $\langle|\mathbf{\Delta}^F(t) - \mathbf{\Delta}_0^F|^2\rangle_r / [\frac{11}{3}C_2(\langle\varepsilon\rangle_0^F \Delta_0^F)^{2/3}]$ versus t for flame particle pairs separated within the inertial range $50\eta \leqslant \Delta_0^F \leqslant 200\eta$ belonging to $T = 500$ K and $T = 1000$ K isosurfaces, respectively.

Clearly, the scaling holds for case B as well, with proportionality constants similar to that observed in case A for $T = 500$ K and $T = 1000$ K, respectively.

Thus, we have observed that despite very different properties of flame and fluid particles, it appears from case A and case B DNS and FPT results shown in Figs. 1 and 2 that their relative dispersion scaling may be quite similar, albeit with different proportionality constants between flame and fluid particles. Following [6] we attempt to analytically investigate the rationale behind such an observation.

The velocity of the ith flame particle is given by

$$\mathbf{V}_i^F(t) = \frac{d}{dt}\mathbf{X}_i^F(t) = \mathbf{U}\left(\mathbf{X}_i^F[t],t\right) + S_d\left(\mathbf{X}_i^F[t],t\right)\mathbf{n}^F\left(\mathbf{X}_i^F[t],t\right). \quad (8)$$

Then the flame particle relative dispersion distance vector $\mathbf{\Delta}^F$ can be defined as

$$\mathbf{\Delta}^F(t) = \mathbf{X}_i^F(t) - \mathbf{X}_j^F(t). \quad (9)$$

Using (8) and (9) we define the flame particle relative dispersion velocity $\mathbf{V}_\Delta^F(t)$:

$$\mathbf{V}_\Delta^F(t) = \mathbf{V}_i^F(t) - \mathbf{V}_j^F(t) = \frac{d\mathbf{\Delta}^F(t)}{dt} \Rightarrow \mathbf{\Delta}^F(t) = \mathbf{\Delta}^F(0) + \int_0^t \mathbf{V}_\Delta^F(t')dt'. \quad (10)$$

Then the dispersion coefficient for flame particles is given by

$$3K_{\text{eff}}^F = \frac{1}{2}\frac{d\langle|\mathbf{\Delta}^F(t)|^2\rangle}{dt} = \left\langle \mathbf{\Delta}^F(t)\frac{d\mathbf{\Delta}^F(t)}{dt}\right\rangle. \quad (11)$$

Putting Eq. (10) in Eq. (11) we get

$$3K_{\text{eff}}^F = \left\langle \mathbf{\Delta}^F(0)\frac{d\mathbf{\Delta}^F(t)}{dt}\right\rangle + \left\langle\left(\int_0^t \mathbf{V}_\Delta^F(t')dt'\right)\mathbf{V}_\Delta^F(t)\right\rangle. \quad (12)$$

Once again using the definition of K_{eff}^F we can write

$$\frac{1}{2}\frac{d\langle|\mathbf{\Delta}^F(t)|^2\rangle}{dt} - \left\langle \mathbf{\Delta}^F(0)\frac{d\mathbf{\Delta}^F(t)}{dt}\right\rangle = \int_0^t \langle\mathbf{V}_\Delta^F(t')\mathbf{V}_\Delta^F(t)\rangle dt'. \quad (13)$$

If t is small, we can approximate the correlation function $\langle\mathbf{V}_\Delta^F(t')\mathbf{V}_\Delta^F(t)\rangle \approx \langle\mathbf{V}_\Delta^F(0)\mathbf{V}_\Delta^F(0)\rangle$ which yields

$$\frac{1}{2}\frac{d\langle|\mathbf{\Delta}^F(t)|^2\rangle}{dt} - \left\langle \mathbf{\Delta}^F(0)\frac{d\mathbf{\Delta}^F(t)}{dt}\right\rangle = \langle\mathbf{V}_\Delta^F(0)\mathbf{V}_\Delta^F(0)\rangle t. \quad (14)$$

Integrating we get $\langle|\mathbf{\Delta}^F(t)-\mathbf{\Delta}^F(0)|^2\rangle = \langle \mathbf{V}^F_\Delta(0)\mathbf{V}^F_\Delta(0)\rangle t^2$.
Now,

$$\begin{aligned}\left\langle \mathbf{V}^F_\Delta(0)\mathbf{V}^F_\Delta(0)\right\rangle &= \left\langle\left|\left[\mathbf{U}^F_i(0)-\mathbf{U}^F_j(0)+S^F_{d,i}(0)\mathbf{n}^F_i(0)-S^F_{d,j}(0)\mathbf{n}^F_j(0)\right]\right|^2\right\rangle \\ \Rightarrow \underbrace{\left\langle \mathbf{V}^F_\Delta(0)\mathbf{V}^F_\Delta(0)\right\rangle}_{L1} &= \underbrace{\left\langle\left|\mathbf{U}^F_i(0)-\mathbf{U}^F_j(0)\right|^2\right\rangle}_{R1}+\underbrace{\left\langle\left|S^F_{d,i}(0)\mathbf{n}^F_i(0)-S^F_{d,j}(0)\mathbf{n}^F_j(0)\right|^2\right\rangle}_{R2} \\ &+ \underbrace{2\left\langle\left[\mathbf{U}^F_i(0)-\mathbf{U}^F_j(0)\right]\left[S^F_{d,i}(0)\mathbf{n}^F_i(0)-S^F_{d,j}(0)\mathbf{n}^F_j(0)\right]\right\rangle}_{R3}. \end{aligned} \tag{15}$$

As shown in Eq. (15) above, the structure functions of $\mathbf{V}_f$; $\mathbf{U}$; $S_d\mathbf{n}$; $\mathbf{U}$ and $S_d\mathbf{n}$ at $t=0$ are identified as $L1$, $R1$, $R2$, and $R3$, respectively. We can also denote $RS = R1+R2+R3$ such that by checking $L1 = RS$ the structure function calculations could be verified.

Figures 3(a) and 3(b) show the variation of $L1$, $R1$, $R2$, $R3$, and RS for $T = 500$ K and $T = 1000$ K, respectively, corresponding to case A. We observe that the compensated structure function $L1$ of $\mathbf{V}_f$ is nearly constant in the inertial range of interest $50\eta \leqslant \Delta^F_0 \leqslant 242\eta$. This structure function is closely followed by the more well-known fluid velocity structure function $R1$. $L1$ closely follows $R1$, as in both cases $R2$ and $R3$ tend to cancel each other due to similarity in magnitude trends, but opposite signs. Similar behavior of the above structure functions is observed for case B, shown in Figs. 4(a) and 4(b) for $T = 500$ K and $T = 1000$ K, respectively.

Therefore the following approximation holds:

$$\left\langle \mathbf{V}^F_\Delta(0)\mathbf{V}^F_\Delta(0)\right\rangle \sim C_F\left(\langle\varepsilon\rangle^F_0\ \Delta^F_0\right)^{2/3}. \tag{16}$$

This leads to

$$\langle|\mathbf{\Delta}^F(t)-\mathbf{\Delta}^F(0)|^2\rangle = C_F\left(\langle\varepsilon\rangle^F_0\ \Delta^F_0\right)^{2/3}t^2, \tag{17}$$

which is the most important finding of this Rapid Communication.

IV. CONCLUSIONS

In this Rapid Communication we find that a modified version of Batchelor's pair dispersion scaling is valid for flame particles. However, unlike for fluid particles in NRIHIT, the proportionality constants for flame particles, C_F, is not universal but depends on the temperature value of the isotemperature surface to which the flame particles belong. The difference or nonuniversality in the coefficients could be attributed to the increased kinematic viscosity and anisotropy effects resulting from gas expansion in the mean flow direction caused by localized heat release due to combustion. Nevertheless, in complex turbulent flows further complicated by chemical reactions, heat release, and dilatation, the existence of such simple scaling laws offers encouraging signs towards possible unified viewpoints.

ACKNOWLEDGMENTS

This work was partially supported by a research grant from the ISRO-IISc Space Technology Cell's sponsored research program (Grant No. ISTC/MAE/SC/334).

[1] G. I. Taylor, Proc. London Math. Soc. **s2–20**, 196 (1922).
[2] L. F. Richardson, Proc. R. Soc. London, Ser. A **110**, 709 (1926).
[3] J. P. L. C. Salazar and L. R. Collins, Annu. Rev. Fluid Mech. **41**, 405 (2009).
[4] A. Obukhov, On the distribution of energy in the spectrum of turbulent flow, Dokl. Akad. Nauk SSSR **32**, 22 (1941).
[5] A. N. Kolmogorov, The local structure of turbulence in incompressible viscous fluid for very large Reynolds numbers, Dokl. Akad. Nauk SSSR **30**, 299 (1941).
[6] G. Batchelor, Q. J. R. Meteorol. Soc. **76**, 133 (1950).
[7] K. R. Sreenivasan, Phys. Fluids (1994–present) **7**, 2778 (1995).
[8] M. Bourgoin, N. T. Ouellette, H. Xu, J. Berg, and E. Bodenschatz, Science **311**, 835 (2006).
[9] G. Damköhler, Z. Elektrochem. **46**, 601 (1940) [NASA Tech. Mem. 1112, 1947].
[10] N. Swaminathan and K. N. C. Bray, *Turbulent Premixed Flames* (Cambridge University Press, Cambridge, 2011).
[11] A. Lipatnikov and J. Chomiak, Prog. Energy Combust. Sci. **28**, 1 (2002).
[12] S. Pope, Int. J. Eng. Sci. **26**, 445 (1988).
[13] S. Girimaji and S. Pope, J. Fluid Mech. **234**, 247 (1992).
[14] P. K. Yeung, S. S. Girimaji, and S. B. Pope, Combust. Flame **79**, 340 (1990).
[15] S. Chaudhuri, Proc. Combust. Inst. **35**, 1305 (2015).
[16] C. K. Law, *Combustion Physics* (Cambridge University Press, New York, 2006).
[17] J. Li, Z. W. Zhao, A. Kazakov, and F. L. Dryer, Int. J. Chem. Kinet. **36**, 566 (2004).
[18] N. Babkovskaia, N. E. L. Haugen, and A. Brandenburg, J. Comput. Phys. **230**, 1 (2011).
[19] See Supplemental Material at http://link.aps.org/supplemental/10.1103/PhysRevE.91.021001 for two movies showing motion of all flame particles on the T = 500 K iso-surface for Case A and B. The figure S1 shows pair dispersion for a particular flame particle pair for Case A.
[20] N. Peters, J. Fluid Mech. **384**, 107 (1999).
[21] S. Chaudhuri, F. Wu, and C. K. Law, Phys. Rev. E **88**, 033005 (2013).